Reports of Practical Oncology and Radiotherapy 25 (2020) 117–124

Available online at www.sciencedirect.com

Reports of Practical Oncology and Radiotherapy

journal homepage: http://www.elsevier.com/locate/rpor

Original research article

Comparison of CT artifacts and image recognition of various fiducial markers including two types of thinner fiducial markers for CyberKnife treatment

Toshihiro Suzuki[a,*], Masahide Saito[b], Hiroshi Onishi[b], Koji Mochizuki[a], Kenichiro Satani[a], Akihiro Yamazaki[c], Kenichi Miura[c], Shinji Taka[d], Naoki Sano[b], Takafumi Komiyama[b], Hiroshi Takahashi[a]

[a] *Kasugai CyberKnife Rehabilitation Hospital, Yamanashi, Japan*
[b] *Department of Radiology, University of Yamanashi, Yamanashi, Japan*
[c] *Shizuoka City Shimizu Hospital, Shizuoka, Japan*
[d] *Shizuoka General Hospital, Shizuoka, Japan*

ARTICLE INFO

Article history:
Received 7 May 2019
Received in revised form 4 September 2019
Accepted 2 December 2019
Available online 9 December 2019

Keywords:
Fiducial marker
CyberKnife
VISICOIL
Gold Anchor
SBRT
CT artifact

ABSTRACT

Aim: The aim of the study was to evaluate computed tomography (CT) artifacts and image recognition of the CyberKnife system. Regarding fiducial markers, VISICOIL of 0.5 mm × 5.0 mm and 0.75 mm × 5.0 mm, ball-shaped Gold Anchor (GA) of 0.28 mm × 10 mm and 0.28 mm × 20 mm, were compared with the standard cylinder marker of 0.9 mm × 3.0 mm (ACCULOC).
Background: Recently, various kinds of commercial fiducial markers have been available in CyberKnife treatment.
Materials and methods: The CT images of a water equivalent gel with each fiducial marker were acquired for the evaluation of CT artifacts. The evaluation was performed using the standard deviation of Hounsfield Unit (HU) value for a rectangle region near the fiducial marker. Then, to evaluate the image recognition, each fiducial marker was located to overlap in the target locating system (TLS) for the two sites; the vertebral bone and the pubic bone.
Results: For CT artifacts, the standard deviations of the VISICOIL of 0.5 mm × 5.0 mm was the smallest. The image recognition of four fiducial markers had a value close to the standard cylinder marker and was feasible for common use, but was slightly poorer when using GA of 0.28 mm × 10 mm in the dynamic conditions.
Conclusion: Our results indicated that VISICOIL 0.5 × 5.0 mm and the GAs can be used nearly always for CyberKnife treatment in spite of their much thinner needles than those of cylinder types.

1. Introduction

Stereotactic body radiotherapy (SBRT) using CyberKnife (Accuray, Sunnyvale, California, USA) has been recently introduced as a treatment modality for tumors outside the central nervous system and is already performed in many institutions. Specifically, CyberKnife involves using a 6 MV linear accelerator mounted on a robotic arm and allows for irradiation from a specified location with six degrees of freedom.[1–3] To deliver treatment, a 2D image can also be acquired at 5–150 seconds inter- and intra-fraction by using two kV X-ray devices (target locating system, TLS), resulting in a high-precision image-guided radiotherapy.[4] In addition, a dynamic tracking method using fiducial markers placed in or around the target is available. SBRT using CyberKnife is particularly effective for the treatment of tumors located in organs with respiratory movement such as the lung or liver. It is also effective for the treatment of the prostate, which moves depending on urine volume in the bladder or gas and feces in the rectum. Various kinds of commercial fiducial markers for radiation treatment are available, namely, VISICOIL (RadioMed Corporation, Bartlett, TN, USA), GA (Naslund Medical AB, Huddinge, Sweden), ACCULOC, Fusioncoil, PolyMark (CIVCO Medical Solutions, Kalona, IA, USA) and Gold

* Corresponding author at: Kasugai CyberKnife Rehabilitation Hospital, 436 Kou, Kasugai-cho, Fuefuki-city, Yamanashi, 406-0014, Japan.
E-mail address: suzuki@kasugai-reha.com (T. Suzuki).

https://doi.org/10.1016/j.rpor.2019.12.005
1507-1367/

Table 1
Characteristics of various kinds of commercial fiducial markers.

Fiducial marker	Coil diameter, mm (needle size (G) or introducer diameter (mm))
VISICOIL (RadioMed Corporation, Bartlett, TN, USA)	0.35 (19 G, 22 G), 0.5 (18 G,19 G, 21 G),[a] 0.75 (18 G),[a] 1.1 (17 G)
Gold Anchor (Naslund Medical AB, Huddinge, Sweden)	0.28 (22 G, 25 G)[a]
ACCULOC (CIVCO Medical Solutions, Kalona, IA, USA)	0.9 (18 G),[a] 1.2 (17 G), 1.6 (14 G)
FusionCoil (CIVCO Medical Solutions, Kalona, IA, USA)	1.0 (18 G)
PolyMark (CIVCO Medical Solutions, Kalona, IA, USA)	1.0 (18 G)
Gold Marker (Olympus Co. Ltd., Tokyo, Japan)	1.5 (1.94 mm)

[a] Our study evaluated the markers.

Marker (Olympus Co. Ltd., Tokyo, Japan). The characteristics of each marker are summarized in Table 1.

However, the clinical use of these fiducial markers for CyberKnife treatment is limited by the following factors (1) poor image recognition in TLS, (2) high degree of invasion such as pneumothorax, bleeding and infection for the marker placement, and (3) artifacts of treatment-planning computed tomography (CT).[5–8] Therefore, each fiducial marker must be sufficiently validated before it can be used in the clinical setting. In general, (1) might be improved with the use of large markers, while (2) and (3) might be improved by using thinner needles and fiducial markers.

Recently, two types of thinner needles have been introduced for CyberKnife treatment: VISICOIL of 0.5 mm × 5.0 mm with 21 G needle and Gold Anchor with 25 G needle. In this study, we evaluated the CT artifacts and image recognition for CyberKnife treatment of four kinds of markers including these two types of fiducial markers compared with those of a standard cylinder marker ACCULOC (0.9 mm × 3.0 mm).

2. Materials and methods

2.1. Characteristics of fiducial markers

Four fiducial markers, the straight-shaped VISICOIL (0.5 mm × 5.0 mm and 0.75 mm × 5.0 mm) and the ball-shaped GA (0.28 mm × 10 mm and 0.28 mm × 20 mm), were evaluated in this study. However, only the ball-shaped GA was evaluated because the straight-shaped type cannot be recognized by the CyberKnife system. The features of these markers were compared with a standard cylinder marker ACCULOC (0.9 mm × 3.0 mm), which has obtained a regulatory approval in Japan, and it is conventionally used in CyberKnife treatment.[9] Fig. 1 shows the appearance of each fiducial marker. The VISICOIL is made of gold (above 99.95 %), 0.35–1.1 mm wide, and 5–30 mm long. Meanwhile, the GA is made of alloy comprising 0.5 % iron and has two types according to the insertion method, namely, ball-shaped and straight-shaped.[10] The ball-shaped is formed by inserting the coil while holding the needle, and the straight-shaped is formed by inserting the coil while pulling the needle. The ACCULOC is made of gold (above 99.99 %). In the TLS system, template matching is performed between a template image reconstructed from the DRR image and the live image on the system. The template image is defined as the expansion of 10 pixels in all directions from the selected part of the fiducial marker. The pixel size of both images is approximately 0.4 mm, indicating that the maximum detection range is approximately 8 mm. Therefore, the fiducial marker of more than 8.0 mm in diameter might be misrecognized on the CyberKnife system. The straight-shaped GA is over 8.0 mm on the TLS system; therefore, only the ball-shaped GA was evaluated in this study.

2.2. Evaluation of CT artifacts

CT artifacts were evaluated for each fiducial marker. First, the CT images of a water equivalent gel (40 mm × 40 mm × 25 mm cylinder-shaped) with each marker were acquired. A water equivalent gel was used to make the same conditions as the body. All CT images were acquired using Optima CT660 (GE Medical Systems, Milwaukee, WI, USA) in the following settings: 120 kV, 400 mA, 1.25-mm slice thickness, 100-mm field of view (FOV), and 512 × 512 pixels. These were the same settings used clinically and in our study, the CT values of the markers were approximately 10 pixels. This feature was the same for all markers. Therefore, a CT slice, which had a maximum standard deviation of the HU value for a region of 30 pixels from the center of the marker (namely, 61 × 61 pixels) as an area where artifacts can be evaluated sufficiently, was selected to evaluate the CT artifacts. For all markers, Wilcoxon signed-rank test was performed. Moreover, the Hounsfield Unit (HU) value of the region of fiducial marker was converted from more than 250 HU to 0 HU to evaluate only the outside region by excluding the high CT value of the fiducial marker. These analyses were performed via MATLAB 2016a (Mathworks, Natick, MA, USA).

2.3. Evaluation of the image recognition of CyberKnife system

To evaluate the accuracy of fiducial tracking of the CyberKnife system, the image recognition of each fiducial marker on TLS was investigated. We used an uncertainty value, which was used in TLS for the evaluation of fiducial tracking. The uncertainty value between the DRR image and the live image was calculated using the Zero-means Normalized Cross-Correlation (ZNCC) which is a similarity index. ZNCC is a general index of image similarity, and the image intensity and X–Y coordinates of DRR image and live image are used for calculation, respectively. ZNCC can range from −1 to 1, and the value is 1 if the two images are matched completely. The analysis was performed in a region of 21 × 21 pixels, which included a fiducial marker. The uncertainty value improved to as close to 0 % as possible, and the threshold of the value is generally set as 40 % in the clinical use of the CyberKnife system.

The image recognition of each fiducial marker in TLS was evaluated under two regions in which the fiducial markers often overlap with the bone in TLS (1) pelvic region and (2) abdominal region.

2.3.1. Pelvis

The fiducial marker is often overlapped in TLS with the pubic bone during CyberKnife treatment to the pelvic region, such as in prostate cancer. Therefore, the evaluation for image recognition under the condition that the fiducial marker is overlapped with the pubic bone in TLS was performed using an in-house phantom (Fig. 2(a) and (b)). Each marker was inserted into the Rand phantom (arrow) on the condition that the marker is overlapped with the pubic bone in TLS (a). Rand phantom was fixed on a vacuum immobilization system for planning CT and verification of overlapping with the pubic bone in TLS (b). Set-up of in-house phantom; the gel with the marker was lifted on the acrylic board, which was attached to a driven stick (c). The Rand phantom was placed under the condition that the fiducial marker was overlapped with the vertebral bone in TLS (d). First, the CT images of the Rand phantom (The Phantom Laboratory, Salem, NY, USA) with each fiducial marker (straight-shaped VISICOIL, ball-shaped GA and ACCULOC) were acquired. A water equivalent gel (5 mm × 5 mm × 12 mm), involving each fiducial marker, was inserted in the Rand phantom near the bone. A water equivalent gel was used to eliminate the cavity in the insert section. The CT scans were performed with Optima CT660, with 120 kV, 400 mA, 1.25-mm slice thickness, 500-mm FOV, and 512 × 512 pixels. The DRR images were

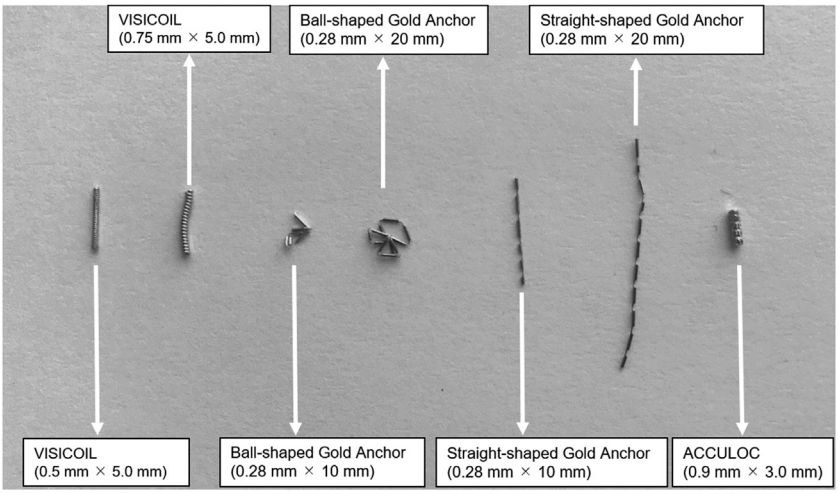

Fig. 1. Fiducial markers used in this study.

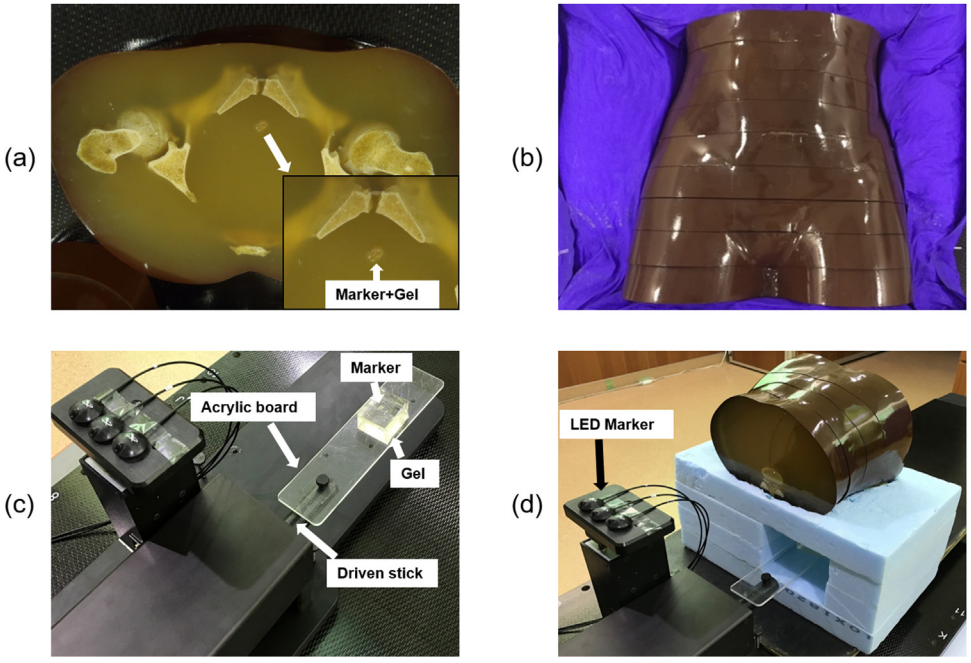

Fig. 2. Experimental set-up of each marker, evaluation of tracking accuracy for the pelvis (a,b), abdomen (c,d), respectively.

generated via the obtained CT images, and treatment beams were created to validate the image recognition for each fiducial marker in TLS.

To acquire live images, X-ray irradiation was performed using the same clinical parameters (120, 130, and 140 kV and 100 and 125 mA with 100 ms exposure time). The uncertainty value was measured ten times.

2.3.2. Abdomen

The fiducial marker is often overlapped in TLS with a vertebral bone during CyberKnife treatment to the abdominal region, such as for liver cancer. For CyberKnife treatment of lung cancer, the Xsight Lung Tracking System is usually used in our institute, which is performed without any other fiducial markers.[11,12] Therefore, in this study, only the abdominal region was evaluated. Moreover, the fiducial marker is applicable regardless of the presence or absence of respiratory movement. Therefore, the evaluation was performed for two kinds of conditions, namely, static and dynamic.

Fig. 2(c) and (d) show the phantom for the evaluation. First, the gel with the marker was lifted on the acrylic board, which was attached to a driven stick. Then, the Rand phantom was placed in such a way that the fiducial marker was overlapped with the vertebral bone in TLS. Irradiation conditions and procedure were the same as in C.1.

For evaluation of the dynamic pattern, a simulate respiration waveform (SI: ± 10 mm; respiration width: AP ± 10 mm; cycle time: 4 s of sine wave) was used to move the fiducial marker from the center of the vertebral bone. The waveform was recognized by the CyberKnife system using the LED markers attached in the phantom. The uncertainty value was measured once at eight points (Fig. 3), which were obtained from the respiration waveform via the CyberKnife system under each of the above irradiation conditions.

In addition, a Wilcoxon signed-rank test was performed using the mean of the uncertainty values obtained in C.1 and C.2 (static and dynamic) to evaluate the image recognition for each marker. All data analyses were performed using the IBM SPSS statistics ver. 24 software (IBM, Armonk, NY, USA).

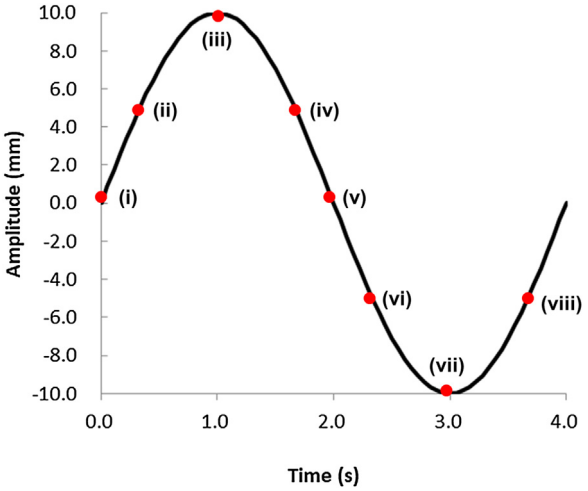

Fig. 3. A respiratory sine wave used in this study. Eight points on the wave are defined.

3. Results

3.1. CT artifacts

Fig. 4 shows the 2D profile curves of the selected CT slice and the standard deviations of the CT value for each marker. The CT slice including the maximum standard deviation was selected as the CT artifact was the most pronounced. The standard deviation was calculated for 61 × 61 pixels near the fiducial marker with converting the region of more than 250 to 0 HU. The standard deviations of the two VISICOILs and two GAs were significantly smaller than that of the ACCULOC ($p < 0.05$). The standard deviations were 120.6, 203.6, 181.1, 205.5, and 441.9 HU for VISICOIL (0.5 mm × 5.0 mm), VISICOIL (0.75 mm × 5.0 mm), GA (0.28 mm × 10 mm), GA (0.28 mm × 20 mm), and ACCULOC (0.9 mm × 3.0 mm), respectively. The standard deviations of the two VISICOILs and two GAs were significantly smaller than that of the ACCULOC ($p < 0.05$).

3.2. Evaluation of the image recognition of the CyberKnife system

3.2.1. Pelvis

For the pelvis phantom with the overlapped region of each marker and the pubic bone, the 2D image acquisitions were performed using TLS under some irradiation conditions. Fig. 5 shows the live images obtained in TLS. All markers (arrows) can be visually confirmed in the images.

The mean values of the uncertainty and each standard deviation for all irradiation conditions in the pubic bone are shown in Table 2. Significant differences were observed between VISICOIL (0.75 mm × 5.0 mm) and ACCULOC (0.9 mm × 3.0 mm) ($p < 0.05$). Significant differences were observed between VISICOIL (0.5 mm × 5.0 mm) and ACCULOC (0.9 mm × 3.0 mm) with the exception of under the following condition: 140 kV/100 mA ($p > 0.05$), while the deviation of the average value was similar in all markers. By contrast, no significant differences were observed between GA (0.28 mm × 10 mm and 0.28 mm × 20 mm) and ACCULOC (0.9 mm × 3.0 mm) ($p > 0.05$).

3.2.2. Abdomen

To evaluate the image recognition for the abdominal region using the phantom with the overlapped region of a marker and a vertebral bone, 2D images were also obtained using TLS under certain irradiation conditions. Fig. 5 shows the live images obtained in TLS, and all markers (arrows) can also be visually confirmed similarly as in *3.2.1*.

The mean values of the uncertainty and each standard deviation for all irradiation conditions to the static phantom in the vertebral bone are also shown in Table 2. There was a significant difference between VISICOIL (0.5 mm × 5.0 mm) and ACCULOC (0.9 mm × 3.0 mm) ($p < 0.05$), and VISICOIL (0.75 mm × 5.0 mm) and ACCULOC (0.9 mm × 3.0 mm) ($p < 0.05$), and GA (0.28 mm × 10 mm) and ACCULOC (0.9 mm × 3.0 mm) ($p < 0.05$) respectively. By contrast, no significant differences between GA (0.28 mm × 20 mm) and ACCULOC (0.9 mm × 3.0 mm) were observed under the following condition: 120 kV/125 mA ($p > 0.05$). For GA (0.28 mm × 20 mm), the deviation of the average VISICOIL (0.75 mm × 5.0 mm) and GA (0.28 mm × 20 mm) were smaller than that of the other markers.

Fig. 6 shows the results of the dynamic conditions. Regarding GA (0.28 mm × 10 mm), the uncertainty values of two points (iii and vii) increased compared with other points. Table 3 shows the detail of the mean uncertainty values for all irradiation conditions of each marker for each respiratory point. The uncertainty values of GA (0.28 mm × 10 mm) at two points (iii and vii) were especially higher than those of other markers. At other points, changes of the uncertainty value of all markers were only minimal, while some points had significant differences.

Table 4
The rate and number of cases where fiducial markers overlapped with the bone in TLS in our institution. 159 cases of all 229 cases (69 %) were eligible.

Treatment site	Patient num.	Overlap num.	Rate (%)
Liver	145	101	70
Prostate	34	32	94
Lymph nodes	20	6	30
Pancreas	16	6	38
Kidney	8	8	100
Adrenal gland	4	4	100
Bile duct	2	2	100
All	229	159	69

Patient num.: The number of patient received with body radiation therapy in our institution; Overlap num.: The number of the markers overlapping with bone in TLS.

4. Discussion

Commercial fiducial markers of various diameters are available not only for CyberKnife, but also for linear accelerators, which is the most commonly used device for external beam radiation. In general, using large markers can improve the image recognition and visibility, but CT artifacts might also increase with the use of lager markers. The GA can be indwelled via a minimally invasive process because it has the thinnest diameter among all commercially available markers, and a 25 G needle can be applied to it. However, the straight-shaped GA is a 10 or 20-mm long marker; thus, straight indwelling cannot be recognized in the CyberKnife system because it tends to misrecognize coils longer than 8.0 mm. Moreover, the position of fiducial markers varies for each patient and treatment site; thus, they do not always provide a high accuracy of image recognition in TLS. In particular, in the event that the thin marker overlaps with the bone in TLS, the image recognition may be significantly decreased. Table 4 shows the rate and number of cases in which the fiducial markers overlapped with the bone in TLS in our institution, which generally occurs in 69 % of overall cases. The ACCULOC with a larger marker diameter (0.9 mm × 3.0 mm) than VISICOIL (0.5 × 5.0 mm, 0.75 mm × 5.0 mm) and GA is sometimes used for CyberKnife treatment. In this study, we investigated image recognition and CT artifacts of two VISICOILs and two GAs compared with the ACCULOC.

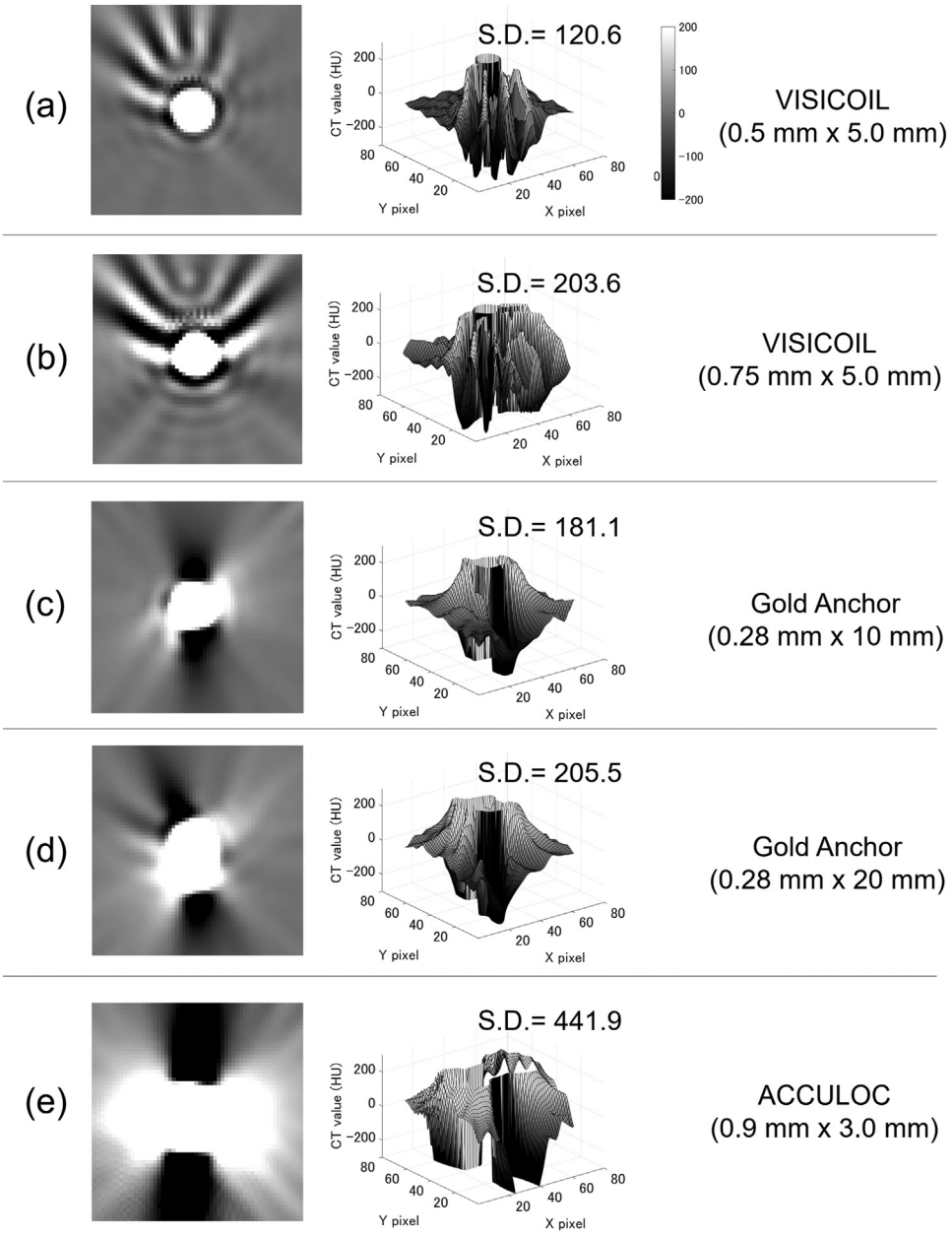

Fig. 4. Comparison of standard deviations of the CT images for each fiducial marker, (a) thorough (e): straight-shaped VISICOIL (0.5 mm × 5.0 mm), straight-shaped VISICOIL (0.75 mm × 5.0 mm), ball-shaped Gold Anchor (0.28 mm × 10 mm), ball-shaped Gold Anchor (0.28 mm × 20 mm) and ACCULOC (0.9 mm × 3.0 mm), respectively.

Table 2
The mean values of uncertainty and each standard deviation for all irradiation conditions to the static phantom (pubic bone and vertebral bone). The position of the marker was overlapped with the pubic bone and center of the vertebral bone in TLS, respectively.

			Uncertainty (%, mean ± S.D.)								
			VISICOIL				Gold Anchor				ACCULOC
Site	kV/ms	mA	0.5 × 5.0 mm	p-value	0.75 × 5.0 mm	p-value	0.28 × 10 mm	p-value	0.28 × 20 mm	p-value	0.9 × 3.0 mm
Pubic bone	120/100	100	15.0 ± 0.4	<0.05	14.8 ± 0.3	<0.05	14.8 ± 0.3	0.11	14.6 ± 0.3	0.11	14.3 ± 0.2
		125	15.0 ± 0.3	<0.05	14.7 ± 0.2	<0.05	14.9 ± 0.3	0.11	14.5 ± 0.3	0.07	14.1 ± 0.2
	130/100	100	15.0 ± 0.3	<0.05	14.9 ± 0.4	<0.05	14.4 ± 0.5	0.11	14.2 ± 0.3	0.34	14.1 ± 0.2
		125	15.0 ± 0.4	<0.05	14.6 ± 0.3	<0.05	14.3 ± 0.3	0.34	14.1 ± 0.2	0.73	14.0 ± 0.2
	140/100	100	14.8 ± 0.4	0.12	14.7 ± 0.2	<0.05	14.3 ± 0.4	1.00	14.1 ± 0.2	1.00	14.0 ± 0.3
		125	14.7 ± 0.4	<0.05	14.6 ± 0.2	<0.05	14.3 ± 0.5	0.51	14.0 ± 0.2	0.18	13.9 ± 0.1
Vertebral bone	120/100	100	21.2 ± 1.0	<0.05	18.0 ± 0.2	<0.05	17.5 ± 0.6	<0.05	17.0 ± 0.2	<0.05	16.5 ± 0.6
		125	21.1 ± 0.8	<0.05	18.1 ± 0.3	<0.05	17.3 ± 0.6	<0.05	17.2 ± 0.2	0.75	16.7 ± 0.9
	130/100	100	20.6 ± 1.1	<0.05	18.0 ± 0.2	<0.05	17.4 ± 0.7	<0.05	17.3 ± 0.2	<0.05	16.2 ± 0.5
		125	20.6 ± 1.0	<0.05	18.2 ± 0.2	<0.05	17.3 ± 0.6	<0.05	17.3 ± 0.2	<0.05	16.2 ± 0.4
	140/100	100	20.2 ± 0.6	<0.05	18.0 ± 0.3	<0.05	17.7 ± 0.5	<0.05	17.2 ± 0.2	<0.05	16.0 ± 0.5
		125	20.0 ± 0.7	<0.05	18.1 ± 0.3	<0.05	17.3 ± 0.8	<0.05	17.0 ± 0.2	<0.05	16.0 ± 0.6

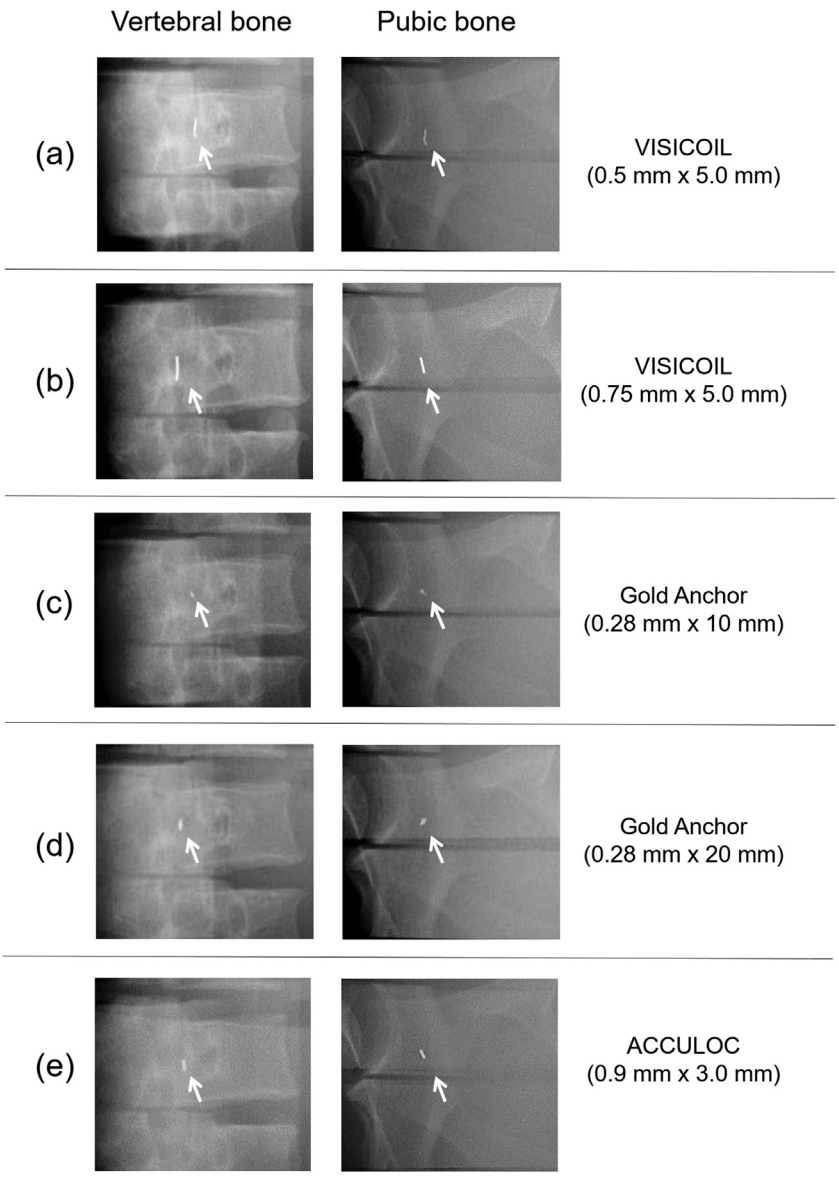

Fig. 5. Fluoroscopic images with each fiducial marker overlapped with the vertebral bone (left) and the pubic bone (right) in TLS. The straight-shaped VISICOIL with 0.5 mm × 5.0 mm, straight-shaped VISICOIL with 0.75 mm × 5.0 mm, ball-shaped Gold Anchor with 0.28 mm × 10 mm, ball-shaped Gold Anchor with 0.28 mm × 20 mm, and ACCULOC (0.9 mm × 3.0 mm) are showed from (a) to (e), respectively (arrow).

Table 3
The mean values of uncertainty and each standard deviation of all irradiation conditions of each marker for eight respiratory points. For the evaluation of the dynamic pattern, simulate respiration waveform (SI: ± 10 mm; respiration width: AP ± 10 mm; cycle time: 4 s of sine wave) was used to move the fiducial marker from the position of center of vertebral bone.

	Uncertainty (%, mean ± S.D.)								
	VISICOIL				Gold Anchor				ACCULOC
Respiratory point	0.5 × 5.0 mm	p-value	0.75 × 5.0 mm	p-value	0.28 × 10 mm	p-value	0.28 × 20 mm	p-value	0.9 × 3.0 mm
i	20.3 ± 1.2	0.22	18.7 ± 2.2	0.69	19.7 ± 2.3	0.69	19.2 ± 0.5	0.69	17.1 ± 3.8
ii	15.4 ± 2.4	0.22	21.0 ± 1.3	0.69	21.7 ± 1.8	0.69	18.7 ± 1.0	0.69	20.1 ± 3.8
iii	18.0 ± 1.6	<0.05	20.5 ± 1.2	<0.05	36.6 ± 1.2	<0.05	20.9 ± 1.2	<0.05	15.7 ± 1.2
iv	14.2 ± 0.8	<0.05	20.6 ± 1.8	1.0	20.9 ± 3.4	0.22	18.3 ± 0.8	1.00	18.3 ± 2.9
v	20.1 ± 1.4	0.22	21.0 ± 2.0	0.22	20.7 ± 5.0	<0.05	19.2 ± 0.7	0.22	14.6 ± 3.8
vi	26.9 ± 0.9	<0.05	20.1 ± 1.7	0.22	27.1 ± 3.4	<0.05	22.0 ± 1.4	<0.05	17.1 ± 1.2
vii	17.3 ± 1.1	1.00	21.3 ± 1.7	<0.05	37.9 ± 2.0	<0.05	16.9 ± 0.7	0.69	17.2 ± 1.5
viii	26.0 ± 1.3	<0.05	21.4 ± 2.5	<0.05	32.1 ± 3.0	<0.05	23.1 ± 1.2	0.22	19.3 ± 1.9

Metal artifacts inhibit accurate image reconstruction, and are the result of a significantly reduced amount of X-ray incident on the detector due to metal having a high X-ray absorption rate. Therefore, large markers absorb more X-rays, which increase artifacts.[13] Due to CT artifacts, inaccuracies in the HU values result in error in electron density or stopping power estimate, which may significantly affect the dose calculation and optimization processes.[14–16] Therefore, it is important to reduce the artifacts. Tanaka et al. evaluated the visibility of CT artifacts relative to the presence of each fiducial marker.[17] For a more detailed investigation, the CT arti-

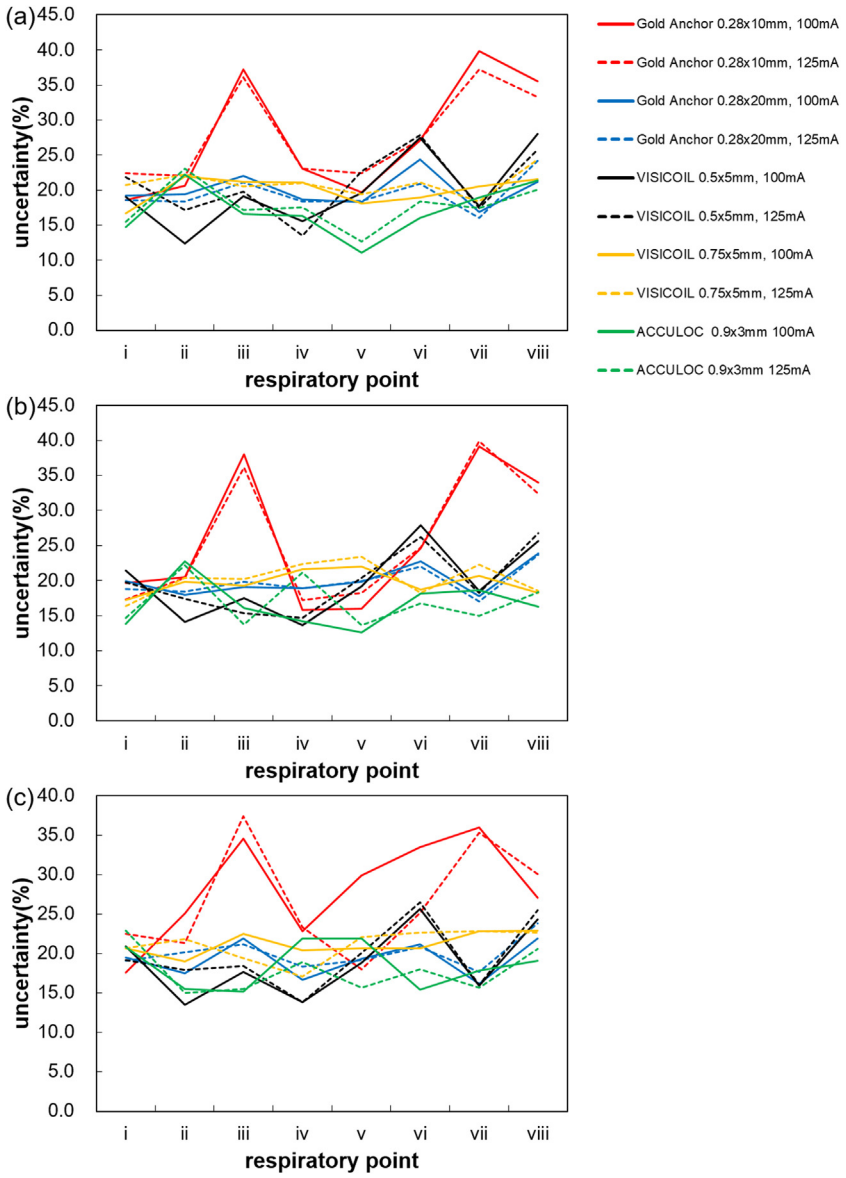

Fig. 6. Values of uncertainty for X-ray irradiation under each condition of each marker at the point of i to viii on respiratory waveform, 120 kV (a), 130 kV (b), 140 kV (c).

facts were quantitatively evaluated in this study. The standard deviations of the two VISICOILs and two GAs were significantly smaller than that of the ACCULOC ($p < 0.05$), indicating that these markers could reduce the metal artifacts compared to the standard cylinder marker. However, the ball-shaped GA also had higher density per pixels of CT images than the straight-shaped VISICOIL (0.5 mm × 5.0 mm); as such, the standard deviations of ball-shaped GA were larger than those of VISICOIL (0.5 mm × 5.0 mm). Furthermore, VISICOIL (0.75 mm × 5.0 mm) had a value close to GA (0.28 mm × 20 mm). Future studies should investigate the fiducial markers under other conditions and investigate their effects on dose distribution.

Regarding image recognition, there have been no studies to evaluate the image recognition of fiducial marker under the difficult tracking conditions in CyberKnife system, while Marsico et al. have evaluated the visibility of markers with the subjective visual evaluation on the CT images.[18] Therefore, we focused on the image recognition of each fiducial marker in CyberKnife treatment.

For the image recognition in the pelvic bone with the overlapped region of each marker in TLS, our results demonstrated that both GA (0.28 mm × 10 mm and 0.28 mm × 20 mm) and ACCULOC can provide better image recognition than VISICOIL (0.5 mm × 5.0 mm and 0.75 mm × 5.0 mm). However, although two VISICOILs had a relatively high uncertainty value, this was not clinically problematic. Therefore, we recommend using VISICOIL (0.5 mm × 5.0 mm) and GA (0.28 mm × 10 mm) among four fiducial markers for treatments in the pelvic region. However, these results were obtained in only one insertion place. In actual treatment, the insertion site, size of the prostate, and position of the prostate vary. As such, the fiducial marker in TLS can be overlapped with not only the pubic bone, but also the ischium and bone cortex. The ischial bone and bone cortex tend to have a higher contrast than the pubic bone used in this study. In addition, the value of uncertainty may change depending on rectal movement and stomach gas. Further studies are needed to evaluate the performance of fiducial markers in these various conditions.

On the other hand, for evaluation at the abdominal region for the static phantom, our results demonstrated that both VISICOIL and GA had high uncertainty values that were not clinically problematic, which was similar to that in the pelvic region. Meanwhile,

for evaluation at the abdominal region for the dynamic phantom, the uncertainty value of GA (0.28 mm × 10 mm) reached up to 40 % near the cortex of the vertebral bone, and this might be because the vertebral bone was thicker than the pubic bone. Another possible reason is that although the GA density (0.28 mm × 10 mm) was increased by rolling, the size of the marker itself became small. Therefore, we recommend using VISICOIL (0.5 mm × 5.0 mm) and GA (0.28 mm × 20 mm) among the four fiducial markers for static and/or dynamic treatments in the abdominal region. However, because a phantom was used in this study, the image recognition of the system and the visibility might change, depending on the body thickness, bone shape, and respiratory wave of the patient. Moreover, the shape of the fiducial marker can vary, depending on the insertion method. Future studies should investigate the fiducial markers under other conditions.

5. Conclusion

In this study, we evaluated the CT artifacts and image recognition on TLS for four fiducial markers; straight-shaped VISICOIL of 0.5 mm × 5.0 mm, straight-shaped VISICOIL of 0.75 mm × 5.0 mm, ball-shaped Gold Anchor (GA) of 0.28 mm × 10 mm and 0.28 mm × 20 mm, in comparison with the standard cylinder marker of 0.9 mm × 3.0 mm (ACCULOC). These four fiducial markers can be used for CyberKnife treatment. In particular, VISICOIL (0.5 mm × 5.0 mm) and GA (0.28 mm × 10 mm, 0.28 × 20 mm) are quite useful in terms of less invasiveness according of their much thinner needles than those of cylinder types. The results of our study can be useful in understanding and selecting the appropriate fiducial marker for clinical CyberKnife treatment.

Financial disclosure

None declared.

Conflict of interest

There are no conflicts of interest to declare.

References

1. Adler Jr JR, Murphy MJ, Chang SD, et al. Image-guided robotic radiosurgery. *Neurosurgery*. 1999;44(6):1299–1306, discussion 306-7.
2. Murphy MJ, Adler JR, Bodduluri M, et al. Image-guided radiosurgery for the spine and pancreas. *Comput Aided Surg*. 2000;5(4):278–288.
3. Murphy MJ, Cox RS. The accuracy of dose localization for an image-guided frameless radiosurgery system. *Med Phys*. 1996;23(12):2043–2049.
4. Mallarajapatna GJ, Susheela SP, Kallur KG, et al. Image guided internal fiducial placement for stereotactic radiosurgery (CyberKnife). *Indian J Radiol Imaging*. 2011;21(1):3.
5. Persson GF, Josipovic M, Nygaard DE, et al. Percutaneously implanted markers in peripheral lung tumours: report of complications. *Acta Oncol (Madr)*. 2013;52(6):1225–1228.
6. Castellanos E, Wersäll P, Tilikidis A, et al. Low infection rate after transrectal implantation of gold anchor™ fiducial markers in prostate Cancer patients after non-broad-spectrum antibiotic prophylaxis. *Cureus*. 2018;10(10).
7. Langenhuijsen JF, van Lin EN, Kiemeney LA, et al. Ultrasound-guided transrectal implantation of gold markers for prostate localization during external beam radiotherapy: complication rate and risk factors. *Int J Radiat Oncol Biol Phys*. 2007;69(3):671–676.
8. Igdem S, Akpinar H, Alco G, et al. Implantation of fiducial markers for image guidance in prostate radiotherapy: patient-reported toxicity. *Br J Radiol*. 2009;82(983):941–945.
9. Challapalli A, McLauchlan R, Robinson A, et al. Implementing image-guided prostate radiotherapy: use of the ACCULOC® system to optimise the planning target volume margins and to assess the potential clinical benefit. *Clin Oncol*. 2012;24(8):590–591.
10. Tanaka O, Nishigaki Y, Hayashi H, et al. The advantage of iron-containing fiducial markers placed with a thin needle for radiotherapy of liver cancer in terms of visualization on MRI: an initial experience of Gold Anchor. *Radiol Case Rep*. 2017;12(2):416–421.
11. Bahig H, Campeau M-P, Vu T, et al. Predictive parameters of CyberKnife fiducial-less (XSight Lung) applicability for treatment of early non-small cell lung cancer: a single-center experience. *Int J Radiat Oncol Biol Phys*. 2013;87(3):583–589.
12. Bibault J-E, Prevost B, Dansin E, et al. Image-guided robotic stereotactic radiation therapy with fiducial-free tumor tracking for lung cancer. *Radiat Oncol*. 2012;7(1):102.
13. Barrett JF, Keat N. Artifacts in CT: recognition and avoidance. *Radiographics*. 2004;24(6):1679–1691.
14. Giantsoudi D, De Man B, Verburg J, et al. Metal artifacts in computed tomography for radiation therapy planning: dosimetric effects and impact of metal artifact reduction. *Phys Med Biol*. 2017;62(8):R49.
15. Habermehl D, Henkner K, Ecker S, et al. Evaluation of different fiducial markers for image-guided radiotherapy and particle therapy. *J Radiat Res*. 2013;54(suppl_1):i61–i68.
16. Reft C, Alecu R, Das IJ, et al. Dosimetric considerations for patients with HIP prostheses undergoing pelvic irradiation. Report of the AAPM Radiation Therapy Committee Task Group 63. *Edical Phys*. 2003;30(6):1162–1182.
17. Tanaka O, Iida T, Komeda H, et al. Initial experience of using an iron-containing fiducial marker for radiotherapy of prostate cancer: advantages in the visualization of markers in Computed Tomography and Magnetic Resonance Imaging. *Polish J Med Phys Eng*. 2016;22(4):93–96.
18. Marsico M, Gabbani T, Livi L, et al. Therapeutic usability of two different fiducial gold markers for robotic stereotactic radiosurgery of liver malignancies: a pilot study. *World J Hepatol*. 2016;8(17):731.